Coupled mechanism of enhanced and inhibitory effects of nanoscale zero-valent iron on methane production and antibiotic resistance genes in anaerobic digestion of swine manure

Tiedong Lu [a, 1], Junya Zhang [b, c, 1], Tianming Su [a], Xuelian Liang [d], Yuansong Wei [b, c], Tieguang He [a, *]

[a] Agricultural Resource and Environment Research Institute, Guangxi Academy of Agricultural Sciences, Nanning, Guangxi, 530007, China

[b] State Key Joint Laboratory of Environmental Simulation and Pollution Control, Research Center for Eco-Environmental Sciences, Chinese Academy of Sciences, Beijing, 100085, China

[c] University of Chinese Academy of Sciences, 100049 Beijing, China

[d] Research Institute of Agro-products Quality Safety and Testing Technology, Guangxi Academy of Agriculture Sciences, Nanning, 530007, Guangxi, China

[1] Tiedong Lu and Junya Zhang contributed equally to this work

[*] **Correspondence:**

Tel.: +86-771-3243829; Fax: +86-771-3243829.

E-mail address: tghe118@163.com (Tieguang He).

Abstract: In this study, the turning point for nanoscale zero-valent iron's (NZVI) promotion and inhibition effects of methane production coupled with the reduction of antibiotic resistance genes (ARGs) was investigated. Adding 150 mmol/L NZVI increased methane production by maximum of 23.8%, which was due to the chemical reaction producing H_2 and enhancement of direct interspecies electron transfer (DIET) by NZVI. NZVI350 dramatically repressed methane generation by 48.0%, which might be associated with the large quantity of reactive oxygen species (ROS) and excessive H_2 inhibiting the functioning of microorganisms. The fate of ARGs was significantly related to daily methane production, indicating that the more methane production finally generated, the less the abundance of ARGs at last left. The reduction of ARGs was enhanced by maximum of 61.0%, which was attributed to the inhibition of vertical gene transfer (VGT) and horizontal gene transfer (HGT) caused by steric hindrance associated with NZVI corrosion.

Keywords: Swine manure, Nanoscale zero-valent iron, Anaerobic digestion, High-throughput qPCR, Antibiotic resistance genes

1. Introduction

Antibiotic resistance genes (ARGs) are becoming more common as a result of increased antibiotic use. ARGs have risen to become among the most serious public health concerns of the twenty-first century (Murray et al., 2022). According to the UK Government-commissioned Review on ARGs, ARGs might kill ten million people per year by 2050 (O'Neill, 2016). The development of ARGs is an important issue that requires a global and coordinated response according to World Health Organization (Van Boeckel et al., 2019). In China, livestock antibiotic use (52% of overall antibiotic use) is considered to be slightly greater than human antibiotic use (48%) (Qiao et al., 2018). However, about 30% ~ 90% of antibiotics remain unabsorbed and are reserved in the urine or feces. Thus, antibiotic residues, as well as antibiotic resistance genes (ARGs), have been commonly identified in livestock waste, making it a significant reservoir of ARGs on an environmental scale (Ji et al., 2012). According to the China's National Bureau of Statistics, the country produced nearly 2.0×10^{12} kg of livestock manure in 2017, with pig wastes accounting for 618 billion kilograms (Wang et al., 2021), and the proper handling of swine manure has become one of the most important aspects of ARG control in the environment.

As a result, the Chinese government implemented the Action Plan for Animal and Poultry Manure Utilization (2017–2020) in 2017 to promote the resources use of poultry and livestock manure, with anaerobic digestion (AD) serving as the principal treatment approach (Ma et al., 2018). AD is widely utilized for both energy generation and waste management, as it converts waste into biogas. In 2017, it was projected that the energy potential of manure-produced biogas was 6.73×10^{12} MJ, accounting for around 5 percent of China's total energy requirements (Wang et al., 2021). As a result, how to boost methane production has become a hot research topic, with a lot of potential for field use. Iron-based compounds are commonly used as flocculants, reductive agents, or Fenton reagents, and considered as non-toxic and low-cost materials (Lizama et al., 2019; Sun et al., 2019; Yuan et al., 2020; Zheng et al., 2022).

Iron-based compounds have been extensively studied and considered as a promising way to improve methane production, eliminate the odorous gas H_2S emissions, and improve phosphate recovery in AD, where zero-valent iron (ZVI) could alter the dominant functional bacteria, improve hydrolysis, and DIET (Dong et al., 2022; Ye et al., 2021; Zhang et al., 2021). Due to ZVI's powerful reductants, they can reduce the oxidation–reduction state in AD, function as a major enzymatic co-factor and electron donor, and provide additional H_2 for H_2-using microbes (Yang et al., 2019, 2018). Meanwhile, ZVI has been shown to promote ARG reduction in AD of swine manure, thermophilic digestion of sewage sludge (Gao et al., 2017; Zhang et al., 2021). In the pervious investigation, a ZVI dosage of 75 mmol/L decreased ARGs by 25.0 %, and particularly diminished inactivation of aminoglycoside resistance genes by antibiotics, as well as antibiotic target protection of tetracycline resistance genes (Zhang et al., 2021). As a result, adding ZVI to the AD can boost production of methane while also lowering ARG levels.

In comparison to ZVI, nanoscale zero-valent iron (NZVI) has the most potential uses in environmental processes because of its strong chemical reducibility, high efficiency, large specific surface, and amounts of H_2 release (Li et al., 2016; Zhang et al., 2022). Inappropriate concentrations of NZVI, on the other hand, could induce a substantial H_2 shock to biological methanogenesis due to rapid corrosion and an abnormally high partial pressure of H_2 (Huang et al., 2016). Besides, the methanogenic process is inhibited by the reactive nanoparticles connected to cell membranes (Kong et al., 2021). Thus, when using NZVI to boost a substrate's batch assays, the appropriate dosage should be established by the substrate's properties. And different forms of anaerobic sludge have varying levels of tolerance to NZVI toxicity, which could have contributed to inconsistencies between investigations. Therefore, the optimum concentrations of NZVI and the response of functional genes linked with methane generation to NZVI should be further investigated in AD of swine manure. Besides, the information on the fate of ARGs in AD of swine manure by NZVI was usually studied through the traditional quantitative PCR (qPCR), where only part of the ARGs was targeted. Whether the role of NZVI on the ARGs fate in AD is random or specifical needs further investigation. Hence,

technology that targets more ARGs, such as high-throughput qPCR (HT-qPCR), as well as metagenomics, should be used to thoroughly analyze the influence of NZVI on the fate of ARGs in AD, as well as the processes behind the reduction generated by NZVI. In addition, it has not been documented if NZVI's promotion and repression of methane generation has a turning point and how to couple the reduction of ARGs in AD of swine manure.

As a result, the research objectives of this study were summarized as follows: (1) Batch experiments with different concentraion of NZVI were set up to clarify the dosage response of the preformance to NZVI and figure out the turning point for the promotion and inhibition effects in AD of swine manure; (2) Clarify the response of both the microbial community and key functional genes to different doses of NZVI in AD of swine manure; (3) Determine whether the role of NZVI on the fate of ARGs in AD is random or specific through the high-throughput qPCR (HT-qPCR) covering 251 kinds of ARGs; (4) Explore the potential mechanisms associated with the role of NZVI on the fate of ARGs frome perspective of virulence factors (VFs), mobile genetic elements (MGEs), metal resistance genes (MRGs) and microbial community. Finally, the turning point for NZVI's enhancement and repression of methane production effects coupled with the ARGs reduction was disccussed in the AD of swine manure.

2. Materials and methods

2.1 Experimental setup

This study used fresh swine manure and inoculums from a big swine farm in Beijing, China. The total solids (TS) and volatile solids than total solids (VS/TS) of the manure were measured as 38.3% and 83.8% (dry basis), respectively, and it was 3.6% and 57.2% for the inoculum sludge. Meanwhile, the pH of swine manure and inoculum sludge were 7.13 and 7.85, respectively. Aladdin Reagent Co. Ltd., China, provided the 99.5% metals base of NZVI (CAS, 1309-37-1; 50nm). The batch assays were developed utilizing the biochemical methane potential test equipment (Bioprocess Control AB, Sweden), which was utilized to calculate the volume of accumulated methane production at 37°C. The ratio of swine manure to inoculum was 3:1 (on the basis of the contents TS), with a final TS of

around 8% (working volume, 400ml). To achieve appropriate mass transfer, the reactor was continually driven by a mixing motor for 1 minute on and 1 minute off. Five treatments were carried out in triplicate using NZVI with final elemental iron concentrations of 0 mmol/L (CK), 5 mmol/L (NZVI5), 75 mmol/L (NZVI75), 150 mmol/L (NZVI150), and 350 mmol/L (NZVI350). Methane production was continuously monitored, and CO_2 as well as H_2S from the biogas were absorbed using a 3M NaOH solution. On days 0, 6, 13, 23, and 38, samples were collected for analysis based on daily methane production.

2.2 Physico-chemical assays

Samples were span at 8000 rpm for 15 minutes before being filtered via a 0.45μm cellulose membrane. The TS was measured by using the part of the sludge is dried to a constant weight at a temperature between 105 °C. The increase in the weight of the crucible represents the TS of the sample. After the TS value is determined a VS test may be performed. The crucible used for TS testing is ignited at 600 °C for 1 hours. The weight loss on the ignition of the solids represents the VS in the sample. The resulting filtrate for volatile fatty acids (VFAs), total chemical oxygen demand (TCOD), proteins, soluble chemical oxygen demand (SCOD), NH_3-N (ammonia nitrogen content index), and polysaccharides were analyzed as previously described (Lu et al., 2019). ICP-OES (Inductively Coupled Plasma Optical Emission Spectrometer) was adopted to assess the concentration of soluble iron in the filtrate, and ion chromatography was used to determine the content of PO_4^{3-} and SO_4^{2-}. The three-dimensional excitation-emission matrix (EEM) analysis were conducted as previously described (Zhang et al., 2019).

2.3 Analyses of bacterial and archaeal communities

For each treatment, isolation of DNA (from 0.4 ml samples) was done in triplicate with the FAST DNA Spin Kit for Soil (MP Biomedicals, USA), then mixed to serve as the representative DNA sample for subsequent analysis. The NanoDrop ND-1000 (NanoDrop, USA) spectrophotometer and 0.8% agarose gel electrophoresis were utilized to evaluate DNA concentration and quality. Before qPCR and HT-qPCR, the recovered DNA was properly measured using the Qubit2.0 DNA detection

kit. The 515F/806R primers were used to examine the organization of the bacterial community. The Arch349F/Arch806R and Arch340F/Arch1000R nest primers were used to analyze the archaeal community structure (Lu et al., 2019).

Sangon Co., Ltd.'s sequencing center performed pair-end Illumina sequencing (Illumina Miseq, USA) (Shanghai, China). To be annotated taxonomically, the Ribosomal Database Project (RDP) classifier was used, and OTUs with relative abundances less than 0.01 percent were excluded. The diversity indices were produced using the Mothur software tool and the filtered dataset. Each sample's clean 16S rRNA gene sequences were uploaded to the NCBI Sequence Read Archive (SRA) under the project number of PRJNA843570.

2.4 Traditional quantitative PCR (qPCR) and High-throughput quantitative PCR (HT-qPCR)

The six functional genes *cel5*, *cel48*, *hydA*, *ACAS*, *dsrA*, and *mcrA* were quantified, respectively, to evaluate the activities of two cellulose degradation types, fermenters, aceticlastic methanogens, SO_4^{2-}reducing bacteria, and all methanogens (Lu et al., 2020). The primers, annealing temperatures, matching amplification efficiency, and detection limits were reported in the literature (Lu et al., 2020). The Wafergen SmartChip Real-time PCR equipment was used to measure the high-throughput qPCR reactions. As mentioned in previous studies, the 296 primer pairs included 16s rRNA, 251 ARGs, 6 pathogens (virulence factors, VFs), 28 mobile genetic elements (MGEs), and 10 metal resistance genes (MRGs). Aminoglycosides, β-lactamase, macrolide-lincosamide-streptogramin (MLSB), chloramphenicol, multidrug, tetracycline, sulfonamide, as well as vancomycin were among the ARGs tested in the 251 ARGs assays (Lu et al., 2020). Six resistance mechanisms were identified among the ARGs (antibiotic target replacement, antibiotic target alteration, antibiotic efflux, antibiotic inactivation, antibiotic target protection, and unknown). The amplification was carried out in a 100 nL reaction system using 1 LightCycler 480 SYBR Green I Master Mix (Roche Inc., USA), 1 ng L-1 BSA, 2 ng L-1 DNA template, Nuclease-free PCR-Grade water, and 1M of each reverse and forward primer (final concentration). Initial denaturation for 10 minutes at 95 °C, 40 cycles of

denaturation for 30s at 95 °C, annealing for 30s at 60 °C, and finally, auto-generated melting curve analysis. The methods for amplification and computation were previously reported (Lu et al., 2020).

2.5 Data analysis

The maximal production potential, as well as the rate were determined via a modified Gompertz model. The DOMFluor toolbox in MATLAB R2016b was used to do a parallel factor (PARAFAC) analysis of the EEM results (MathWorks, MA). Through the PAST 3.0, the Mantel test revealed connections between microbial communities and ARGs. The between-groups OTU differences ($p < 0.05$) were computed using STAMP 2.1.3, and the ternary plot was created using the ggtern package in R to display the strikingly enriched OTUs. Through Procrustes analysis and Principal component analysis (PCA), the Canoco 5.0 was utilized to examine relationships between measured biological and chemical data. The Spearman correlation established by the Gephi platform (https://gephi.org/) was used to build the network. The correlation matrix was completed using PAST 3.0 and AMOS (SPSS Inc., Chicago, IL, USA) to conduct the structural equation model (SEM) analysis. Prediction of gene functions of microbial communities was conducted by PICRUSt based on the Galaxy platform against the KEGG database (Langille et al., 2013).

3. Results and Discussion

3.1 Dual character of the NZVI on methane production

In comparison to the CK, the NZVI addition had a significant impact on the dynamics of methane generation by the paired sample *t*-test ($p<0.01$). While the effects of NZVI on methane production are not dose-dependent compared with the ZVI addition (Zhang et al., 2021). Adding NZVI75 and NZVI150 increased the accumulative methane production by 21.4% and 23.8%, respectively, from 227.2 mL CH_4 $g^{-1}VS_{add}$ (CK) to 275.8 mL $g^{-1}VS_{add}$ and 2280.6 mL $g^{-1}VS_{add}$, respectively. However, when the dosage was above 350 mmol/L (NZVI350), NZVI significantly inhibited methane production ($p<0.01$). In comparison to CK, the cumulative methane production decreased by 48.0%, from 227.2 mL CH_4 $g^{-1}VS_{add}$ (CK) to 118.0 mL CH_4 $g^{-1}VS_{add}$ (Figure 1a). Methane production increased primarily during peak periods of 5–10 days and 15–28 days (Figure 1b). It was reported

that the first peak is formed by the breakdown of easily degradable organic matter, whereas the second peak is formed by the decomposition of complex organic matter in AD of swine manure (Wu et al., 2017). Furthermore, the addition of NZVI extends the duration of methane production in the second peak, resulting in an increase of methane production. Therefore, the addition of NZVI may promote the degradation of refractory organic matter. According to Gompertz model analysis, the daily maximum methane production rate (R_m) of NZVI150 was significantly increased by 18.7% compared with the CK (Table 1). Although the cumulative methane production of the NZVI350 treatment group was inhibited, it did not inhibit the R_m (Table 1).

As an important intermediate product in AD, VFAs play a pivotal role. The total VFAs in the five groups increased significantly on D6, mainly due to the degradation and conversion of macromolecular substances (for instance polysaccharides and proteins) into VFAs at this stage, where the production rate was greater relative to the consumption rate. Subsequently, due to the quick consumption by the methanogens, VFAs decreased rapidly at D13-D23. The VFA residues in D13-D23 were much smaller than those in the CK group, when the NZVI addition level was less than NZVI350, indicating that an appropriate amount of NZVI promoted the degradation of VFAs. Due to thermodynamic barriers to the degradation of valerate and propionate, they accumulated as AD progressed (D23). However, when adding less than NZVI350, the degradation of valerate and propionate can be promoted. At the end of AD (D38), the addition of appropriate NZVI promoted rapid degradation of propionate compared with CK and NZVI350 groups. In addition, the NZVI350 inhibited the utilization of VFAs. The EEMs data also clearly demonstrated the NZVI addition increased organic decomposition (see supplementary material), and PARAFAC analysis illustrated that the boost was linked to soluble microbial by-products at D6-D13 as well as tyrosine-like compounds throughout the AD process, whose breakdown was dramatically accelerated after adding NZVI less than 150 mmol (Figure. 1d and see supplementary material). The changes in EEMs and VFAs results both indicated the enhancement of the organic degradation through the appropriate NZVI addition (Figure 1c and d).

The TS of each group decreased with the progress of AD, but as the NZVI itself could not be degraded in AD, leading to the higher TS compared with the CK group. Because adding NZVI stimulated the degradation of organic matter, VS/TS was lower than CK after the addition of NZVI, and the decrease of VS/TS increased along with the amounts of NZVI addition (see supplementary material). The pH value was much higher relative to the CK group due to the addition of NZVI and was also proportional to the dosage of NZVI, which was due to the serious corrosion of NZVI in the process of AD (Eqs. (1)-(3)). The removal efficiency of VS (20.9% vs 32.7%), TCOD (31.8% vs 46.1%), SCOD (12.3% vs 51.7%), and proteins (20.1% vs 28.4%) were all improved during the AD, despite minimal change in polysaccharide and ammonia content (see supplementary material). NZVI addition largely increased the concentration of free ammonia (FAN), where the concentration of FAN was increased by 6 times for NZVI350, and this was closely associated with the increase of pH caused by the NZVI addition. These data illustrated that AD systems with higher amounts of NZVI (NZVI350) addition could face the problems of ammonia inhibition, which could inhibit the AD systems. Interestingly, the level of soluble iron in this study increases with the addition of NZVI in the whole AD process, but the concentration of soluble iron increases dramatically only at the end of AD in previous study after adding ZVI (Zhang et al., 2021). This indicated that the iron release was stronger than the iron precipitation in the AD system after adding NZVI, because NZVI has stronger reducing properties than ZVI. The PO_4^{3-} (phosphate) decreased sharply due to the addition of NZVI, which might be associated with the change of the concentration of soluble iron (Eqs. (5)). Because the concentration of SO_4^{2-} was shallow during swine manure AD, the addition of NZVI had a limited impact on SO_4^{2-} alterations. E-supplementary data for this work can be found in e-version of this paper online.

$$Fe^0 + 2H_2O \rightarrow Fe^{2+} + H_2 + 2OH^- \quad (1)$$

$$4Fe^0 + SO_4^{2-} + 4H_2O \rightarrow 3Fe^{2+} + FeS + 8OH^- \quad (2)$$

$$4Fe^0 + CO_2 + 8H^+ \rightarrow CH_4 + 4Fe^{2+} + 2H_2O \quad (3)$$

$$Fe^{2+} + H_2S \rightarrow FeS + 2H^+ \quad (4)$$

$$Fe^{2+} + PO_4^{3-} \rightarrow Fe_3(PO_4)_2 \quad (5)$$

$$Fe^{2+} + CO_2 + H_2O \rightarrow Fe_2CO_3 + 2H^+ \quad (6)$$

$$Fe^{2+} + 2H_2O \rightarrow Fe(OH)_2 + 2H^+ \quad (7)$$

3.2 Effects of NZVI addition on key functional genes

The 16s rRNA (about 10^{11} gene copies μg^{-1} DNA) was greatly reduced in the AD process after adding NZVI, which reflected the biomass change (see supplementary material). NZVI has been illustrated to harbor bactericidal properties considering that NZVI corrosion products can gain entry into microbial cells, then damage the cellular structure (Gao et al., 2017). Previous research has shown that NZVI exposure causes a considerable reduction in the microbial biomass of activated sludge (Wu et al., 2013). This indicated that the iron release (Eqs. (1)-(3)) was stronger than the iron precipitation (Eqs. (4)-(7)) in the AD system after adding NZVI in this study. Furthermore, the appropriate Fe^{2+} and H_2 produced during corrosion may have facilitated the proliferation of functioning microbes, which help the improvement of methane production.

The gene copies of targeted functional genes were reduced after NZVI was added throughout the AD process, which could be due to cellular structural damage induced via iron corrosion, while the dynamics of the *cel5* genes increased at D6-D13 (Figure 2). The activity of glycoside hydrolase genes in cellulose-decomposing bacteria was measured using the *cel5* and *cel48* genes (Pereyra et al., 2010). At D6-D13, NZVI addition increased the gene copies of *cel5*, implying that NZVI supplementation may promote anaerobic cellulose degradation. Despite the fact that *cel48* gene copies were reduced, it was considered that *cel5* may encompass a wider range of anaerobic degraders of cellulose (Pereyra et al., 2010). The H_2-producing bacteria are represented by the *hydA* gene, which encodes the Fe-hydrogenase (Pereyra et al., 2010). The NZVI addition could greatly elevate the H_2 levels in the AD system via corrosion, but NZVI inhibited the H_2 production of *hydA*, and the

inhibition degree was proportional to the NZVI addition, which indicated the high concentration of H_2 may repress the activity of *hydA*. The gene copies of *dsrA* (about 10^5 gene copies g^{-1} DW) were also decreased, and the inhibition degree was also proportional to the NZVI addition, which encodes the dissimilatory sulfite reductase and was linked to the reduction of sulfate reduction in the AD system (Pereyra et al., 2010). This is why the addition of NZVI had a limited impact on SO_4^{2-} alterations.

The gene copies of *ACAS* were also decreased, and the reduction degree was proportional to the NZVI addition in the whole AD process. The *ACAS* was associated with the acetyl-coA synthetase, which denotes acetoclastic methanogenesis and exhibited the potential for acetoclastic methanogenesis (Aydin et al., 2015). The change in *mcrA* was the same as the change in *ACAS*, which coded for the methyl coenzyme M reductase active, indicating methanogenesis in the AD system, covering both hydrogenotrophic and acetoclastic methanogens (Aydin et al., 2015). These illustrated that a higher level of NZVI could repress methanogenesis by decreasing the gene copies of *ACAS* and *mcrA*. Interestingly, only the relative abundance of *ACAS*/*mcrA* was enriched on D6-D13 for the change in relative abundance of function genes, indicating that NZVI addition could improve methane production by increasing hydrogenotrophic rather than acetoclastic methanogenesis in the early stage of AD. Nonetheless, other target genes changed little for the change in relative abundance of function genes compared with the absolute abundance after NZVI addition (see supplementary material).

3.3 Promotion of ARGs reduction via addition of NZVI

NZVI addition improved the reduction of ARGs, and there were about 53–125 subtypes of ARGs discovered in each sample. The number of ARGs detected was reduced from 71 to 54 following NZVI addition (Figure 3B). The impact of NZVI on the fate of ARGs varied a lot different stages of AD. NZVI increased the abundance of ARGs on D13, although NZVI could reduce the relative abundance of ARGs on D6 and D38 (Figure 3B). The ARGs were divided into 5 groups to assess the impacts of NZVI on antibiotic resistance mechanisms, consisting of antibiotic efflux, antibiotic target replacement, antibiotic target alteration, antibiotic inactivation, antibiotic target protection, as well as

unknown. Antibiotic inactivation, antibiotic efflux, antibiotic target protection, and antibiotic target alteration were the predominant resistance mechanisms, accounting for 34.5%, 33.0%, 20.3%, and 8.8%, respectively (Figure 3A). Through adding NZVI350, the total ARGs reduction was enhanced by 61.0%, and the resistance mechanism of antibiotic efflux, antibiotic inactivation, as well as antibiotic target protection ARGs was reduced by 53.0%, 66.8%, and 82.3%, respectively (Figure 3B). When NZVI was added at 5-150 mmol, the augmentation of ARGs reduction was not markedly improved, in contrast to methane generation.

The most prominent ARGs were tetracycline (41%), MLSB (26%), and aminoglycoside (24%) in the AD of swine manure, which may be due to antibiotic application in pig farming (see supplementary material). AD has limited impact on the reduction of ARGs, but the addition of NZVI can promote ARG reduction, and the NZVI350 can reduce the main ARGs of tetracycline, aminoglycoside, and MLSB by 77.4%, 61.0%, and 24.8%, respectively. The NZVI5, NZVI75, and NZVI350 increased the reduction of total ARGs by 15.6%, 0.60%, and 60.9%, respectively, but the NZVI150 enriched the ARGs by 24.7% and increased the accumulative methane production by a maximum of 21.5% (Figure 3C).

The predominant ARG subtypes were *ermF*, *aadE*, *tetT*, *tetM*, *aphA3-01*, *tetW-01*, etc., and the *ermF* dominance in the AD of swine manure has been extensively confirmed (Lu et al., 2020; Zhang et al., 2021). The dominant ARG subtypes were all effectively reduced except the *tetP*, *mecA*, and *aadD*, which were slightly increased after NZVI350 addition (Figure 3C). The effective decrease of MLSB resistance genes was linked to the reduction of *ermF*, and *ermT-01*, *ermT-02*, and *ermB*, which belong to the antibiotic target alteration. Nevertheless, the rise in aminoglycoside as well as tetracycline resistance genes in AD was a result of an increase in the prevalence of *aadE*, *tetT*, *tetM-02*, *tetM-01*, *aphA3-01*, *tetW-01*, *tetQ*, *aphA3-02*, *sat4*, *tetX*, and *aadD*, and these ARG subtypes belonged to antibiotic inactivation as well as antibiotic target protection. The enrichment of *matA/mel* and *floR* belonged to the antibiotic efflux in AD was reduced after adding NZVI350. These data

indicated that NZVI reduced the relative abundance of total ARGs through the reduction of ARGs that were enriched in AD without NZVI addition.

Although the AD process could reduce the MGEs, MRGs, and VFs, the addition of NZVI has a limited impact (Figure 3D). The main enriched MRG was *czcA* (with Co/Zn/Cd resistance), and the main enriched MGE was *intI-1* with integrase mechanisms after adding NZVI (Figure 3D). Nonetheless, the MGEs of transposase mechanisms were decreased after adding NZVI and were proportional to the NZVI addition.

3.4 Alterations in bacterial and archaeal community response to NZVI

Microbial community diversity decreased in general as AD progressed, and NZVI had a negative impact on the diversity indexes (see supplementary material). The two most prevalent phylum in the AD system were Bacteroidetes and Firmicutes, with Firmicutes (63.3%–88.1%) outnumbering Bacteroidetes (11.5%–78.1%). The abundance of Firmicutes was increased along with AD, and the addition of the NZVI promoted the increase. *Bacteroidetes* abundance at D5 was boosted by NZVI addition, whereas the opposite trend was observed at D13-D38 (see supplementary material).

PCA analysis indicated that microbial community changes could be stratified into three stages and that NZVI350 markedly changed community compositions at D13 and D38 ($p < 0.05$; Figure 4A). The three stages corresponded to the hydrolysis, acetogenesis, and methanogenesis phases of AD. The top five genera are *Clostridium sensu stricto*, *unclassified_"Bacteroidales"*, *unclassified_Ruminococcaceae*, *unclassified_Clostridiales*, and *Terrisporobacter* during the whole AD period (Figure 4B). These were the most common fermenters in AD, and they were thought to be necessary degraders of the macromolecular compounds involved in the AD process. *Clostridium sensu stricto* was prevalent throughout the AD process, which was linked to its wide range of functions. *Clostridium sensu stricto* was a fermentation bacterium that degraded macromolecules and produced both alcohol and acid (Peng et al., 2018), which increased after adding NZVI in AD, but NZVI350 decreased the abundance at D13, perhaps resulting in low organic matter degradation rates at D13-D38 with the NZVI350 addition.

The ternary plot indicated the enriched genera were unclassified_"*Bacteroidales*", *Bacteroides*, *Anaerococcus* at the early stage (D6) (Figure 4C). It was reported that *Bacteroidales* were often responsible for the hydrolysis, which degraded proteins, polysaccharides, and lipids into glucose and amino acids, as well as VFAs and quantities of H_2 and CO_2, which were concentrated at D6 with the rise of VFAs (Li et al., 2018). However, NZVI350 significantly reduced the abundance of *unclassified_"Bacteroidales"* at D13, so high dose NZVI may inhibit the degradation of organic matter by reducing its abundance, which is congruent with the trend of COD and methane production. *Bacteroides* have been linked to cellulose degradation, which corresponded well with a decrease in the relative abundance of functional genes *cel48* (Hupfauf et al., 2018). The *Anaerococcus* should have been introduced to the AD system by swine manure, but they were unable to adapt, and their relative abundance declined over time (Zhang et al., 2019). Its relative abundance was 7.5% at D0, but it was only 0.20% at the end (D38).

Propionate accumulated on D13, and the AD system was inhibited, as shown by the reduction of daily methane production. The *Clostridium III* and *Alkaliflexus* were enriched at D13. *Clostridium* could create a syntrophic metabolism with methanogens to boost methane synthesis in addition to degrading complex organics (Peng et al., 2018). The abundance of *Clostridium III* was significantly decreased after adding NZVI350, which decreased from 6.17% to 1.44% at D13 and decreased from 4.34% to 0.2% at D38 compared with CK. This well explains the inhibition of methane production along with AD after adding NZVI350. *Alkaliflexus* was found to aid cellulose degradation, and propionate was the primary fermentation product in AD, which explained its role in D13 under propionate accumulation (Zhao et al., 2018). The NZVI addition increased *Alkaliflexus* abundance at D6. Still, it exhibited an opposite tendency on D13 and D38, especially for NZVI350, which was consistent with the change of propionate in AD.

Unclassified *Clostridiales*, unclassified *Clostridia*, and *Syntrophomonas* were the enriched genus on D38, and *Syntrophomonas*, as the key syntrophic bacteria, can not only engage in the breakdown of long-chain fatty acids but additionally metabolize syntrophy with methanogens (Sousa

et al., 2007). Furthermore, it could manufacture methane not only with hydrogenotrophic methanogens and H_2 and CO_2, but also together with acetoclastic methanogens and DIET. *Syntrophomonas* was significantly decreased from 1.84% to 0.37% after adding NZVI350 at D38. However, the addition of NZVI less than 350mmol/L had a limited effect on its abundance, which was in accordance with the inhibition of propionate and methane production.

Throughout the AD process, *Methanosarcina*, *Methanosphaera*, and *Methanoculleus* were the most prevalent archaea genera, accounting for 65.6%, 12.7%, and 9.9%, respectively. (Figure 4D). At D6, the dominant archaea was *Methanosarcina*, which can utilize acetate, monomethylamine, methanol, dimethylamine, H_2/CO_2, trimethylamine, as well as CO for methane production and is correlated with DIET in the AD system (Capson-Tojo et al., 2018). The NZVI addition increased the abundance of *Methanosarcina* but decreased the abundance of *Methanosphaera*. *Methanosphaera* has one of the most restricted-energy metabolisms compared with the *Methanosarcina*, and it depends on acetate as the primary carbon source for growth and utilizes H_2 to repress methanol to produce methane (Capson-Tojo et al., 2018). Along with AD (D13), the genus of *Methanosphaera* continues to decrease, but *Methanosarcina* has increased, and the NZVI addition promoted the abundance of *Methanosarcina*. The methane production increased remarkably when the addition of NZVI was less than 350 mmol/L because the high concentration of NZVI led to the serious corrosion that produced abundant hydrogen and inhibited the utilization of VFAs in the process of AD. At the end of AD, *Methanosphaera* was largely reduced, while *Methanosarcina* and *Methanoculleus* became dominant. The NZVI addition could increase the relative abundance of *Methanosarcina* and decrease the relative abundance of *Methanoculleus*, which showed a similar trend with *Syntrophomonas* when the addition of NZVI was less than 350 mmol/L. *Syntrophomonas* and *Methanosarcina* had a significant correlation ($p < 0.01$), indicating that syntrophy with methanogens plays a crucial role in the later stages of AD. PICRUSt can predict bacterial metabolic functions by comparing the 16S rRNA gene sequence to a microbial reference genome database with the known metabolic functions. The prediction of the second level of metabolism pathways in different groups by the KEGG PATHWAY

Database (see supplementary material). As can be seen, the abundance of Membrane Transport, Energy Metabolism, amino acid metabolism, and carbohydrate metabolites were higher than other metabolism pathways. This may be related to the microbial activities and the large amounts of soluble carbohydrate and soluble protein solubilization in swine manure. The microbial community structure in the NZVI350 groups has changed at D13 and D38, so did the pathways of Translation, Xenobiotics Biodegradation and Metabolism, Folding, Sorting and Degradation, Metabolism, and Cellular Processes and Signaling were inhibited at D38, which indicated that the high concentration of NZVI might change these metabolic pathways and further lead to the inhibition of methane production. While the pathway of Metabolism and Cellular Processes and Signaling was enhanced after adding NZVI150, indicating the well-dosed NZVI could promote methane production.

3.5 Mechanisms of the dual character of methane production response to NZVI

The effects of NZVI on methane production are not dose-dependent compared with the zero valent iron (ZVI) addition. The addition of NZV75 has nearly the same effect as adding NZVI150. However, when the dosage was 350 mmol/L (NZVI350), NZVI significantly inhibited methane production by 48.0% ($p<0.01$). Because of the high reducibility of NZVI compared with ZVI, NZVI has an aggressive chemical reaction that can produce large volumes of H_2. The corrosion-triggered H_2 was then used to boost methane production while simultaneously raising the pH of the AD system (Eq1). At D0-D6, the abundant H_2 was easily produced after adding NZVI, resulting in an increasing promotion of methane production. At this stage, NZVI addition increased the abundance of *Methanosarcina* but decreased the abundance of Methanosphaera, which could utilize the H_2 to promote methane production. Conversely, NZVI addition promoted the abundance of fermentative bacterial species, which produced enough of VFAs to provide a lot of precursors for methanogenesis. At D13, an abundance of H_2 was consumed, which led to the H_2 partial pressure being lower relative to the limiting value for the VFAs. Meanwhile, the Methanosarcina was increased continuously, which further led to the production of higher methane production. NZVI has stronger reducing properties than ZVI, a high level of NZVI (NZVI350) with a large specific surface area is remarkably

reactive and could release more H_2 (Eqs. (1)), causing a remarkable H_2 shock to the AD system, and thus decreasing the methane production. In addition, *unclassified_Clostridia* was increased after adding NZVI, which mainly generates acetic as well as butyric acids when degrading organic matter (Yu et al., 2016). But *unclassified_"Bacteroidales"* were showing the opposite trend (Figure 4), which was associated with the propionic fermentation-type (Tan et al., 2012). As a result, NZVI increased butyric acid fermentation, and the VFA composition was optimized at this stage. Therefore, high H_2 buildup restricts methanogenesis after adding NZVI350 on D23, resulting in methane production being completely suppressed. Whereas hydrogenotrophic methanogens may use H_2, an appropriate increase in H_2 generation contributes to the enhancement of methanogenesis. Moreover, *Syntrophomonas* was significantly decreased from 1.84% to 0.37% after adding NZVI350 at D38, which was in accordance with the inhibition of propionate and methane production.

The fact that NZVI introduced a lot of soluble Fe into the system illustrated that the iron release (Eqs. (1)-(3)) was greater than the iron precipitation (Eqs. (4)-(7)) in the AD system, and the microbial community was altered remarkably in response to NZVI, especially between D13 and D38. These findings illustrat that nutritional elements have a function in the AD system. After adding NZVI to the AD system, the hydrogenotrophic methanogens were enhanced, and DIET was enhanced with the increase of *Methanosarcina*, *Clostridium*, and *Syntrophomonas*. There are many reasons for suppression after adding NZVI350. Firstly, NZVI particles can bind to the surfaces of microbial cells and maybe generate a large amount of reactive oxygen species (ROS), which will either directly or indirectly destroy the cell structure, resulting in cell lysis and microbial cell death, thereby significantly reducing cumulative methane production (Wu et al., 2020; Zhong et al., 2022). On the other hand, the level of FAN increased rapidly due to the increase in pH, where the FAN even increased to reach 1658 mg/L for NZVI 350, 6 times higher than the CK. These led to the complete repression of methane production after D13 (Duan et al., 2012).

3.6 Decoding the improvement of ARGs reduction response to NZVI

The impact of NZVI on the fate of ARGs varied a lot at different stages of AD. NZVI increased the relative abundance of ARGs on D13, although NZVI could reduce the relative abundance of ARGs on D6 and D38. NZVI increased the reduction of tetracycline (77.4%) and aminoglycoside resistance genes (61.0%), particularly antibiotic target protection for the tetracycline resistance genes as well as antibiotic inactivation for aminoglycoside resistance genes. The mantel test exhibited a strong correlation between the fate of ARGs and microbial communities (MC, p = 0.00104), MGEs (p = 0.0001), MRGs (p = 0.0003), and pathogens (VF, p = 0.0001). But the correlation between the fate of ARGs and environmental variables (physico-chemical parameters) (EV, p = 0.3582) and functional genes (FG, p = 0.1226) was insignificant. Thus, SEM was used to find out more about the relationship between ARG and these factors (Hu et al., 2016). SEM results revealed that MC and MGEs were the major factors responsible for the alterations in ARGs generated by the addition of NZVI to the AD system (Figure 5A). Furthermore, the MC and MGEs primarily affected ARG change through direct effects, which indicated that the NZVI addition might affect the change of ARGs by inducing the changes of the MC by NZVI. Procrustes analysis was used to further analyze the contribution of MC and MGEs to the changes of ARGs, which indicated that 37.0% and 58.9% of the variables in ARGs were explained by MC and MGEs, respectively (Figure 5B). Furthermore, ARG changes were significantly related to daily methane production (see supplementary material), indicating that the more methane produced, the fewer ARGs remained. At D6, the daily methane production varied little among groups. The ARGs were reduced by the chemical reaction (Zhang et al., 2021). At D13, the DIET was enriched after adding NZVI, which led to more activity of the microbial community and the enrichment of the ARGs. At the end of AD, the addition of appropriate NZVI enhanced the methane production, which could lead to a limited reduction of ARGs. However, due to the high H_2 buildup and production of a large amount of ROS, the microbial activity associated with methanogenesis is restricted after adding NZVI350, leading to the significant reduction of ARGs.

The two basic molecular routes for environmental dissemination of ARG are vertical gene transfer (VGT), as well as horizontal gene transfer (HGT) (Ma et al., 2019; Martinez, 2009). In terms

of VGT, ARGs developed along with their bacterial hosts' proliferation. ARGs can be disseminated across bacteria of the same or different species via transformation, conjugation, and transduction, and then grow alongside their bacterial hosts via VGT. However, the corrosion products of NZVI can gain entry into microbial cells, then damage the cellular structure (Gao et al., 2017), leading to inhibiting of the VGT. On the other hand, accumulated iron corrosion products by excessive NZVI, such as FeS, may encapsulate bacterial cells form steric hindrance, inhibit the DIET, and cause microbial activity associated with VGT and HGT to be inhibited. Furthermore, NZVI might possibly produce a large amount of ROS, which compounds with antibiotics and lowers the selection pressures placed on bacterial hosts that carry ARGs (Wang et al., 2016).

Changes in the microbial community may reflect the transmission of ARGs through the VGT. Network analysis further revealed the significance of VGT for the spread of ARGs (Figure 6A). ARG hosts were identified using network analysis on the basis of spearman correlation ($p<0.01$, $R^2>0.5$), and 77 different genus were discovered to be possible ARG hosts. There are 333 edges related to ARG and MC in the network analysis result. The NZVI addition markedly affected the abundance of ARGs by changing the microbial community at D13 and D38. *Clostridium III*, *Pseudomonas*, *unclassified_Pseudomonadaceae*, *Thiopseudomonas*, *unclassified_Planococcaceae*, *Ignatzschineria*, and *Succinivibrio* were the main hosts of ARGs. The abundance of *Clostridium III* decreased from 6.17% to 1.44% at D13 and decreased from 4.34% to 0.2% at D38 compared with CK. The dynamic changes of *tetG-02* and *tetM-01*, etc. for the tetracycline resistance genes were significantly correlated with *Clostridium III*, which was decreased after adding NZVI. The abundance of *Pseudomonas* and *Succinivibrio* decreased from 0.01% to 0.005% and decreased from 0.38% to 0.13 after adding NZVI350 at D38, which were the hosts of *ermT-02*, *sul2*, and *tetG-02*, etc.. This well explains the reduction of ARGs at the end of AD after adding NZVI350. Besides, network analysis at the subtype level could show the importance of MGEs, MRGs, and VFs in the changes of ARGs (Figure 6B). The edges of the ARG associated with MGEs, MRGs, and VFs in the network analysis were 1220, 299, and 143, respectively. Compared with other variables, the edges of the ARG associated with

MGEs account for 73.4% of all variables, which indicates that MGEs played a more important role in the HGT of ARGs. There were also significantly positive correlations between MRGs (*copA*, *tcrB*, *merA*, *arsA*, *pbrT*) and ARGs, which indicated that there existed multiple resistances in microorganisms. The *22SrDNA*, *uidA*, and *ompA* representing the three pathogens were found to be closely associated with many ARG subtypes. These findings suggest that while HGT was the main factor affecting the change of ARGs, other factors such as MC, VFs, and MRGs should not be neglected. E-supplementary data for this work can be found in e-version of this paper online.

4. Conclusions

NZVI increased the accumulative methane production by a maximum of 23.8%, which was due to chemical reaction and DIET caused by NZVI. However, NZVI350 significantly inhibited methane production by 48.0%, and it was hypothesized that the inhibition could be closely associated with the generation of large amounts of ROS and excessive H_2. The ARGs reduction was enhanced by 61.0%, which was mainly related to aminoglycoside resistance genes of antibiotic inactivation and tetracycline resistance genes of antibiotic target protection. These were attributed to the steric hindrance caused by iron corrosion, which inhibited the VGT and HGT.

Acknowledgements

This work was financially supported by the National Natural Science Foundation of China (51808540), the Fund of Guangxi Academy of Agricultural Sciences (2021YT038) and the Found of Guangxi Agricultural Science and Technology Innovation Alliance (202213).

Conflict of interest

The authors declare no conflict of interest.

Reference

1. Aydin, S., Ince, B., Ince, O., 2015. Application of real-time PCR to determination of combined effect of antibiotics on Bacteria, Methanogenic Archaea, Archaea in anaerobic sequencing batch reactors. Water Res. 76, 88–98. https://doi.org/10.1016/j.watres.2015.02.043
2. Capson-Tojo, G., Trably, E., Rouez, M., Crest, M., Bernet, N., Steyer, J.P., Delgenès, J.P., Escudié, R., 2018. Methanosarcina plays a main role during methanogenesis of high-solids food waste and cardboard. Waste Manag. 76, 423–430. https://doi.org/10.1016/j.wasman.2018.04.004
3. Dong, D., Kyung, O., Woo, J., 2022. Influence of the continuous addition of zero valent iron (ZVI) and nano-scaled zero valent iron (nZVI) on the anaerobic biomethanation of carbon dioxide. Chem. Eng. J. 430, 132233. https://doi.org/10.1016/j.cej.2021.132233
4. Duan, N., Dong, B., Wu, B., Dai, X., 2012. High-solid anaerobic digestion of sewage sludge under mesophilic conditions: Feasibility study. Bioresour. Technol. 104, 150–156. https://doi.org/10.1016/j.biortech.2011.10.090
5. Gao, P., Gu, C., Wei, X., Li, X., Chen, H., Jia, H., Liu, Z., Xue, G., Ma, C., 2017. The role of zero valent iron on the fate of tetracycline resistance genes and class 1 integrons during thermophilic anaerobic co-digestion of waste sludge and kitchen waste. Water Res. 111, 92–99. https://doi.org/10.1016/j.watres.2016.12.047
6. Hu, H.W., Wang, J.T., Li, J., Li, J.J., Ma, Y.B., Chen, D., He, J.Z., 2016. Field-based evidence for copper contamination induced changes of antibiotic resistance in agricultural soils. Environ. Microbiol. 18, 3896–3909. https://doi.org/10.1111/1462-2920.13370
7. Huang, Y.X., Guo, J., Zhang, C., Hu, Z., 2016. Hydrogen production from the dissolution of nano zero valent iron and its effect on anaerobic digestion. Water Res. 88, 475–480. https://doi.org/10.1016/j.watres.2015.10.028

8. Hupfauf, S., Plattner, P., Wagner, A.O., Kaufmann, R., Insam, H., Podmirseg, S.M., 2018. Temperature shapes the microbiota in anaerobic digestion and drives efficiency to a maximum at 45 °C. Bioresour. Technol. 269, 309–318. https://doi.org/10.1016/j.biortech.2018.08.106
9. Ji, X., Shen, Q., Liu, F., Ma, J., Xu, G., Wang, Y., Wu, M., 2012. Antibiotic resistance gene abundances associated with antibiotics and heavy metals in animal manures and agricultural soils adjacent to feedlots in Shanghai; China. J. Hazard. Mater. 235–236, 178–185. https://doi.org/10.1016/j.jhazmat.2012.07.040
10. Kong, X., Niu, J., Zhang, W., Liu, J., Yuan, J., Li, H., Yue, X., 2021. Mini art review for zero valent iron application in anaerobic digestion and technical bottlenecks. Sci. Total Environ. 791, 148415. https://doi.org/10.1016/j.scitotenv.2021.148415
11. Langille, M.G.I., Zaneveld, J., Caporaso, J.G., McDonald, D., Knights, D., Reyes, J.A., Clemente, J.C., Burkepile, D.E., Vega Thurber, R.L., Knight, R., Beiko, R.G., Huttenhower, C., 2013. Predictive functional profiling of microbial communities using 16S rRNA marker gene sequences. Nat. Biotechnol. 31, 814–821. https://doi.org/10.1038/nbt.2676
12. Li, L., Hu, J., Shi, X., Fan, M., Luo, J., Wei, X., 2016. Nanoscale zero-valent metals: a review of synthesis, characterization, and applications to environmental remediation. Environ. Sci. Pollut. Res. 23, 17880–17900. https://doi.org/10.1007/s11356-016-6626-0
13. Li, W., Khalid, H., Zhu, Z., Zhang, R., Liu, G., Chen, C., Thorin, E., 2018. Methane production through anaerobic digestion: Participation and digestion characteristics of cellulose, hemicellulose and lignin. Appl. Energy 226, 1219–1228. https://doi.org/10.1016/j.apenergy.2018.05.055
14. Lizama, A.C., Figueiras, C.C., Pedreguera, A.Z., Ruiz Espinoza, J.E., 2019. Enhancing the performance and stability of the anaerobic digestion of sewage sludge by zero valent iron nanoparticles dosage. Bioresour. Technol. 275, 352–359. https://doi.org/10.1016/j.biortech.2018.12.086

15. Lu, T., Zhang, J., Li, P., Shen, P., Wei, Y., 2020. Enhancement of methane production and antibiotic resistance genes reduction by ferrous chloride during anaerobic digestion of swine manure. Bioresour. Technol. 298, 122519. https://doi.org/10.1016/j.biortech.2019.122519
16. Lu, T., Zhang, J., Wei, Y., Shen, P., 2019. Effects of ferric oxide on the microbial community and functioning during anaerobic digestion of swine manure. Bioresour. Technol. 287, 121393. https://doi.org/10.1016/j.biortech.2019.121393
17. Ma, J., Gu, J., Wang, X., Peng, H., Wang, Q., Zhang, R., Hu, T., Bao, J., 2019. Effects of nano-zerovalent iron on antibiotic resistance genes during the anaerobic digestion of cattle manure. Bioresour. Technol. 289, 121688. https://doi.org/10.1016/j.biortech.2019.121688
18. Ma, S., Fang, C., Sun, X., Han, L., He, X., Huang, G., 2018. Bacterial community succession during pig manure and wheat straw aerobic composting covered with a semi-permeable membrane under slight positive pressure. Bioresour. Technol. 259, 221–227. https://doi.org/10.1016/j.biortech.2018.03.054
19. Martinez, J.L., 2009. Environmental pollution by antibiotics and by antibiotic resistance determinants. Environ. Pollut. 157, 2893–2902. https://doi.org/10.1016/j.envpol.2009.05.051
20. Murray, C.J., Ikuta, K.S., Sharara, F., Swetschinski, L., Robles Aguilar, G., Gray, A., Han, C., Bisignano, C., Rao, P., Wool, E., Johnson, S.C., Browne, A.J., Chipeta, M.G., Fell, F., Hackett, S., Haines-Woodhouse, G., Kashef Hamadani, B.H., Kumaran, E.A.P., McManigal, B., Agarwal, R., Akech, S., Albertson, S., Amuasi, J., Andrews, J., Aravkin, A., Ashley, E., Bailey, F., Baker, S., Basnyat, B., Bekker, A., Bender, R., Bethou, A., Bielicki, J., Boonkasidecha, S., Bukosia, J., Carvalheiro, C., Castañeda-Orjuela, C., Chansamouth, V., Chaurasia, S., Chiurchiù, S., Chowdhury, F., Cook, A.J., Cooper, B., Cressey, T.R., Criollo-Mora, E., Cunningham, M., Darboe, S., Day, N.P.J., De Luca, M., Dokova, K., Dramowski, A., Dunachie, S.J., Eckmanns, T., Eibach, D., Emami, A., Feasey, N., Fisher-Pearson, N., Forrest, K., Garrett, D., Gastmeier, P., Giref, A.Z., Greer, R.C., Gupta, V., Haller, S., Haselbeck, A., Hay, S.I., Holm, M., Hopkins, S., Iregbu, K.C., Jacobs, J., Jarovsky, D., Javanmardi, F.,

Khorana, M., Kissoon, N., Kobeissi, E., Kostyanev, T., Krapp, F., Krumkamp, R., Kumar, A., Kyu, H.H., Lim, C., Limmathurotsakul, D., Loftus, M.J., Lunn, M., Ma, J., Mturi, N., Munera-Huertas, T., Musicha, P., Mussi-Pinhata, M.M., Nakamura, T., Nanavati, R., Nangia, S., Newton, P., Ngoun, C., Novotney, A., Nwakanma, D., Obiero, C.W., Olivas-Martinez, A., Olliaro, P., Ooko, E., Ortiz-Brizuela, E., Peleg, A.Y., Perrone, C., Plakkal, N., Ponce-de-Leon, A., Raad, M., Ramdin, T., Riddell, A., Roberts, T., Robotham, J.V., Roca, A., Rudd, K.E., Russell, N., Schnall, J., Scott, J.A.G., Shivamallappa, M., Sifuentes-Osornio, J., Steenkeste, N., Stewardson, A.J., Stoeva, T., Tasak, N., Thaiprakong, A., Thwaites, G., Turner, C., Turner, P., van Doorn, H.R., Velaphi, S., Vongpradith, A., Vu, H., Walsh, T., Waner, S., Wangrangsimakul, T., Wozniak, T., Zheng, P., Sartorius, B., Lopez, A.D., Stergachis, A., Moore, C., Dolecek, C., Naghavi, M., 2022. Global burden of bacterial antimicrobial resistance in 2019: a systematic analysis. Lancet 399, 629–655. https://doi.org/10.1016/S0140-6736(21)02724-0

21. O'Neill, J., 2016. Tackling drug-resistant infections globally: final report and recommendations., The review on antimicrobial resistance. https://doi.org/10.4103/2045-080x.186181

22. Peng, H., Zhang, Y., Tan, D., Zhao, Z., Zhao, H., Quan, X., 2018. Roles of magnetite and granular activated carbon in improvement of anaerobic sludge digestion. Bioresour. Technol. 249, 666–672. https://doi.org/10.1016/j.biortech.2017.10.047

23. Pereyra, L.P., Hiibel, S.R., Prieto Riquelme, M. V., Reardon, K.F., Pruden, A., 2010. Detection and quantification of functional genes of cellulosedegrading, fermentative, and sulfate-reducing bacteria and methanogenic archaea. Appl. Environ. Microbiol. 76, 2192–2202. https://doi.org/10.1128/AEM.01285-09

24. Qiao, M., Ying, G.-G., Singer, A.C., Zhu, Y.-G., 2018. Review of antibiotic resistance in China and its environment. Environ. Int. 110, 160–172. https://doi.org/https://doi.org/10.1016/j.envint.2017.10.016

25. Sousa, D.Z., Smidt, H., Madalena Alves, M., Stams, A.J.M., 2007. Syntrophomonas zehnderi sp. nov., an anaerobe that degrades long-chain fatty acids in co-culture with Methanobacterium formicicum. Int. J. Syst. Evol. Microbiol. 57, 609–615. https://doi.org/10.1099/ijs.0.64734-0
26. Sun, H., Ni, P., Angelidaki, I., Dong, R., Wu, S., 2019. Exploring stability indicators for efficient monitoring of anaerobic digestion of pig manure under perturbations. Waste Manag. 91, 139–146. https://doi.org/10.1016/j.wasman.2019.05.008
27. Tan, H.Q., Li, T.T., Zhu, C., Zhang, X.Q., Wu, M., Zhu, X.F., 2012. Parabacteroides chartae sp. nov., an obligately anaerobic species from wastewater of a paper mill. Int. J. Syst. Evol. Microbiol. 62, 2613–2617. https://doi.org/10.1099/ijs.0.038000-0
28. Van Boeckel, T.P., Pires, J., Silvester, R., Zhao, C., Song, J., Criscuolo, N.G., Gilbert, M., Bonhoeffer, S., Laxminarayan, R., 2019. Global trends in antimicrobial resistance in animals in low- And middle-income countries. Science (80-.). 365. https://doi.org/10.1126/science.aaw1944
29. Wang, H., Yao, H., Sun, P., Li, D., Huang, C.H., 2016. Transformation of Tetracycline Antibiotics and Fe(II) and Fe(III) Species Induced by Their Complexation. Environ. Sci. Technol. 50, 145–153. https://doi.org/10.1021/acs.est.5b03696
30. Wang, Y., Zhang, Y., Li, J., Lin, J.G., Zhang, N., Cao, W., 2021. Biogas energy generated from livestock manure in China: Current situation and future trends. J. Environ. Manage. 297, 113324. https://doi.org/10.1016/j.jenvman.2021.113324
31. Wu, D., Shen, Y., Ding, A., Mahmood, Q., Liu, S., Tu, Q., 2013. Effects of nanoscale zero-valent iron particles on biological nitrogen and phosphorus removal and microorganisms in activated sludge. J. Hazard. Mater. 262, 649–655. https://doi.org/10.1016/j.jhazmat.2013.09.038
32. Wu, J., Hu, Y., Wang, S., Cao, Z., Li, H., Fu, X.-M., Wang, K., Zuo, J., 2017. Effects of thermal treatment on high solid anaerobic digestion of swine manure: Enhancement assessment and kinetic analysis. Waste Manag. 62, 69–75. https://doi.org/10.1016/j.wasman.2017.02.022

33. Wu, Y., Wang, S., Liang, D., Li, N., 2020. Conductive materials in anaerobic digestion: From mechanism to application. Bioresour. Technol. 298, 122403. https://doi.org/10.1016/j.biortech.2019.122403
34. Yang, Y., Wang, J., Zhou, Y., 2019. Enhanced Anaerobic Digestion of Swine Manure by the Addition of Zero-Valent Iron. Energy and Fuels 33, 12441–12449. https://doi.org/10.1021/acs.energyfuels.9b02498
35. Yang, Y., Yang, F., Huang, Weiwei, Huang, Wenli, Li, F., Lei, Z., Zhang, Z., 2018. Enhanced anaerobic digestion of ammonia-rich swine manure by zero-valent iron: With special focus on the enhancement effect on hydrogenotrophic methanogenesis activity. Bioresour. Technol. 270, 172–179. https://doi.org/10.1016/j.biortech.2018.09.008
36. Ye, W., Lu, J., Ye, J., Zhou, Y., 2021. The effects and mechanisms of zero-valent iron on anaerobic digestion of solid waste: A mini-review. J. Clean. Prod. 278, 123567. https://doi.org/10.1016/j.jclepro.2020.123567
37. Yu, B., Huang, X., Zhang, D., Lou, Z., Yuan, H., Zhu, N., 2016. Response of sludge fermentation liquid and microbial community to nano zero-valent iron exposure in a mesophilic anaerobic digestion system. RSC Adv. 6, 24236–24244. https://doi.org/10.1039/c6ra02591a
38. Yuan, T., Bian, S., Hac, J., Liu, J., Shi, X., Xu, Q., 2020. Exploring the roles of zero-valent iron in two-stage food waste anaerobic digestion. Waste Manag. 107, 91–100. https://doi.org/10.1016/j.wasman.2020.04.004
39. Zhang, D., Wei, Y., Wu, S., Zhou, L., 2022. Consolidation of hydrogenotrophic methanogenesis by sulfidated nanoscale zero-valent iron in the anaerobic digestion of food waste upon ammonia stress. Sci. Total Environ. 822, 153531. https://doi.org/10.1016/j.scitotenv.2022.153531
40. Zhang, Junya, Lu, T., Shen, P., Sui, Q., Zhong, H., Liu, J., Tong, J., Wei, Y., 2019. The role of substrate types and substrate microbial community on the fate of antibiotic resistance genes

during anaerobic digestion. Chemosphere 229, 461–470. https://doi.org/10.1016/j.chemosphere.2019.05.036

41. Zhang, J., Lu, T., Wang, Z., Wang, Y., Zhong, H., Shen, P., Wei, Y., 2019. Effects of magnetite on anaerobic digestion of swine manure: Attention to methane production and fate of antibiotic resistance genes. Bioresour. Technol. 291, 121847. https://doi.org/10.1016/j.biortech.2019.121847
42. Zhang, J., Lu, T., Zhong, H., Shen, P., Wei, Y., 2021. Zero valent iron improved methane production and specifically reduced aminoglycoside and tetracycline resistance genes in anaerobic digestion. Waste Manag. 136, 122–131. https://doi.org/10.1016/j.wasman.2021.10.010
43. Zhang, S., Ma, X., Xie, D., Guan, W., Yang, M., Zhao, P., Gao, M., Wang, Q., Wu, C., 2021. Adding activated carbon to the system with added zero-valent iron further improves anaerobic digestion performance by alleviating ammonia inhibition and promoting DIET. J. Environ. Chem. Eng. 9, 106616. https://doi.org/10.1016/j.jece.2021.106616
44. Zhao, Z., Li, Y., Yu, Q., Zhang, Y., 2018. Ferroferric oxide triggered possible direct interspecies electron transfer between Syntrophomonas and Methanosaeta to enhance waste activated sludge anaerobic digestion. Bioresour. Technol. 250, 79–85. https://doi.org/10.1016/j.biortech.2017.11.003
45. Zheng, S., Yang, F., Huang, Wenli, Lei, Z., Zhang, Z., Huang, Weiwei, 2022. Combined effect of zero valent iron and magnetite on semi-dry anaerobic digestion of swine manure. Bioresour. Technol. 346, 126438. https://doi.org/10.1016/j.biortech.2021.126438
46. Zhong, Y., He, J., Zhang, P., Zou, X., Pan, X., Zhang, J., 2022. Effects of different particle size of zero-valent iron (ZVI) during anaerobic digestion: Performance and mechanism from genetic level. Chem. Eng. J. 435, 134977. https://doi.org/10.1016/j.cej.2022.134977

Table 1. Results of the fitting of the modified Gompertz model. *

Treatments	R^2	R_m (mL/ (g VS_{added})	P (mL/g VS_{added})
CK	0.988	9.69	230.35
NZVI5	0.982	10.73	245.67
NZVI75	0.99	10.86	282.45
NZVI150	0.994	11.5（18.7%）	294.96
NZVI350	0.981	11.48	119.39

*The number in the brackets indicated the extent of the improvement by the addition of NZVI compared to the control. R_m is the maximum specific methane production rate (mL d^{-1} g-VSadded^{-1}); P is the bio-methane production potential (mL d^{-1}·g-$VS_{added}{}^{-1}$).

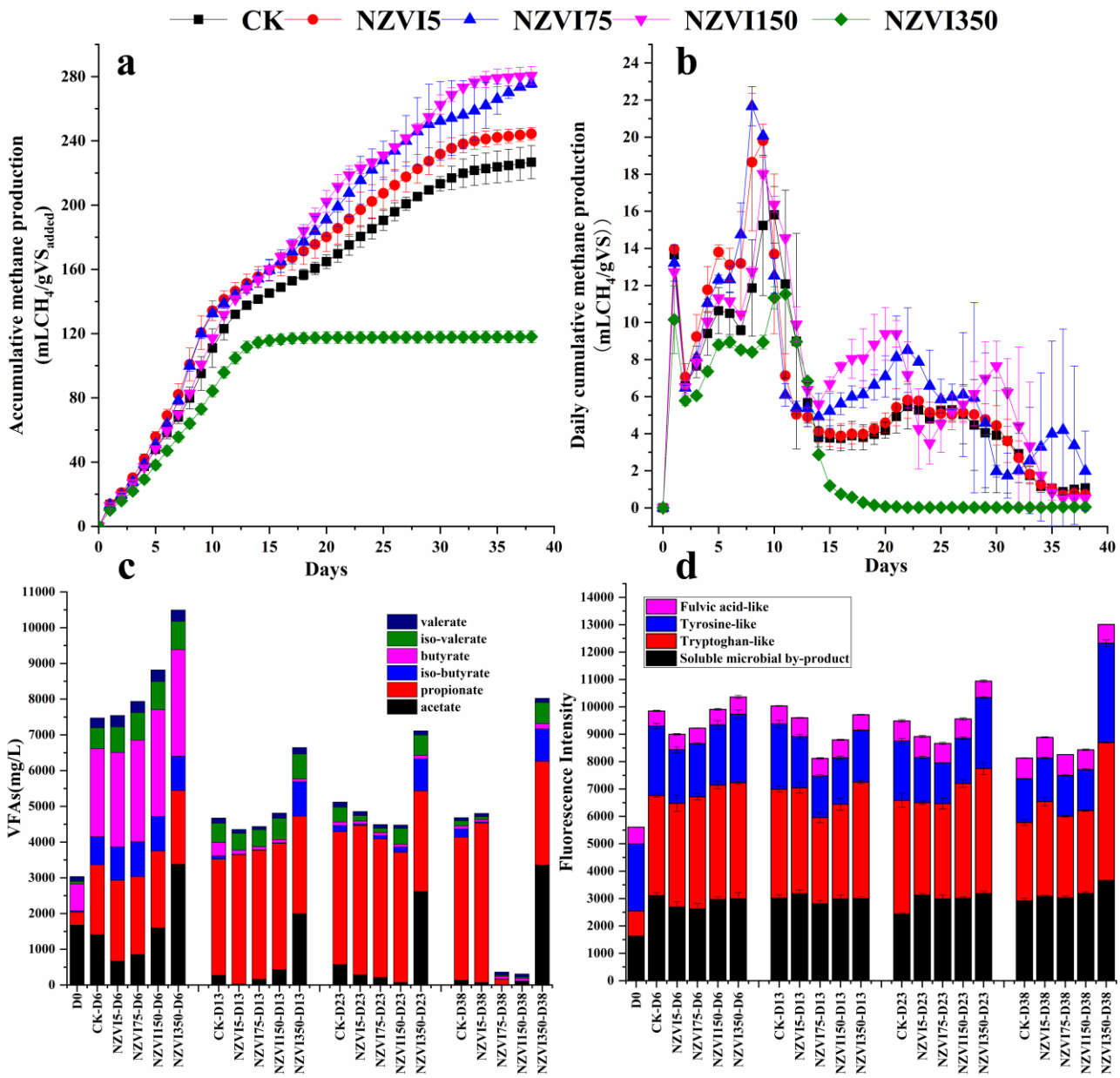

Figure 1. Cumulative methane production (a), daily methane production (b), changes in the concentration of volatile fatty acids (VFAs) (c), and dynamic changes in the fluorescence intensity of the detected components (d) in response to NZVI addition in the AD.

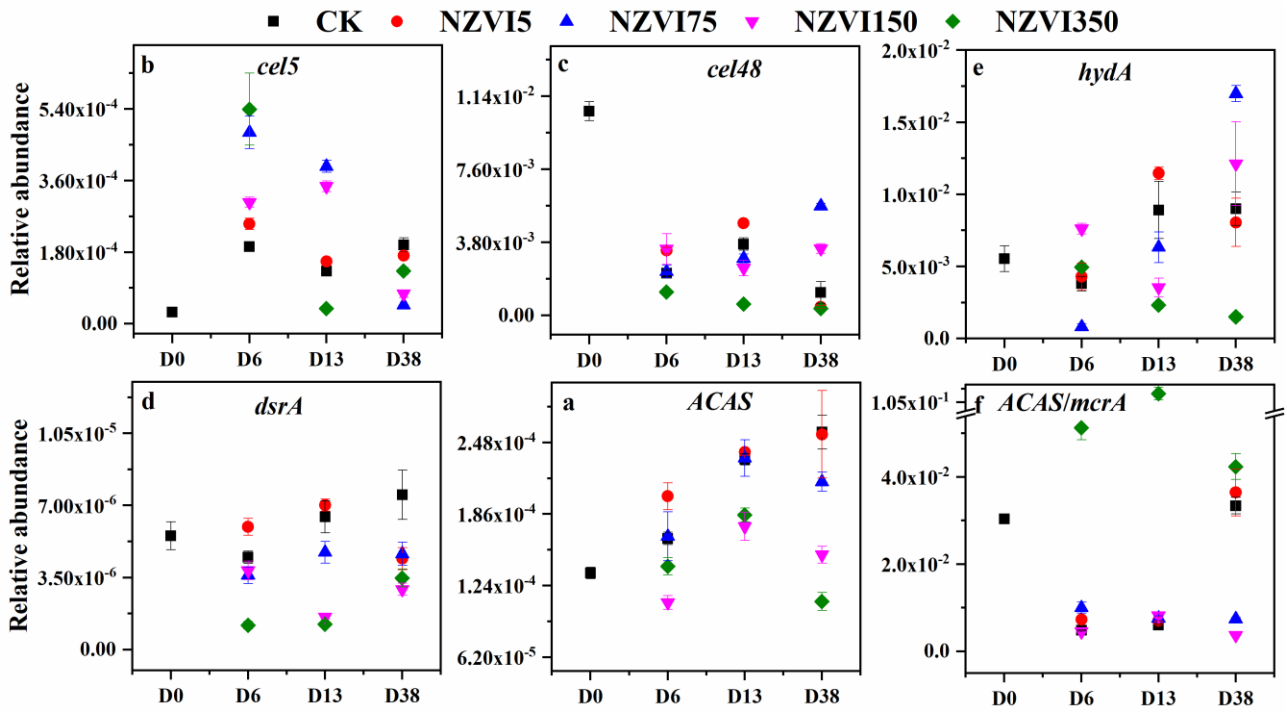

Figure 2. Changes of the functional gene response to NZVI addition in AD of swine manure.

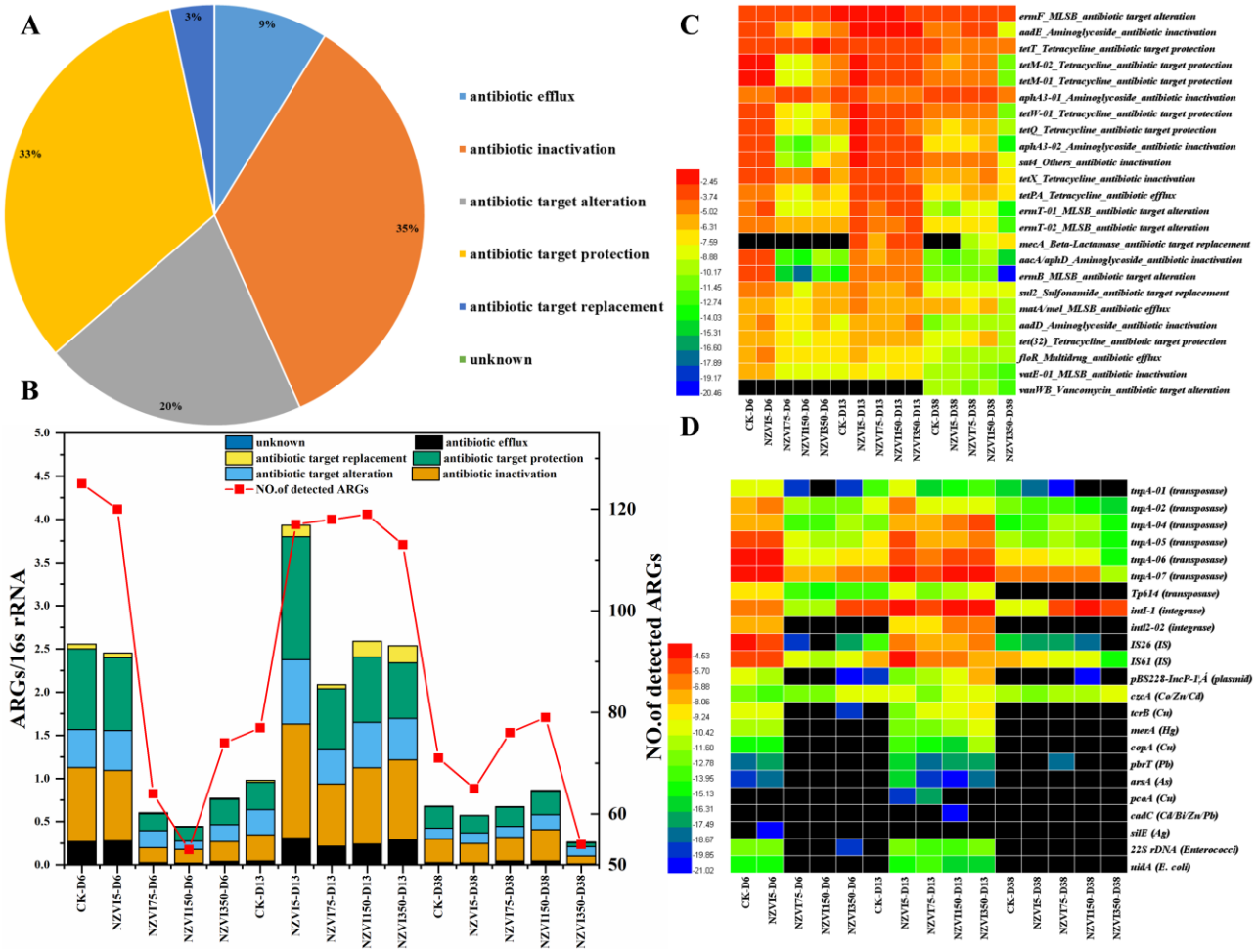

706

707 **Figure 3.** The total distribution of ARGs according to antibiotic resistance mechanisms (A); The

708 changes of antibiotic resistance mechanism (B); Heatmap showing the changes of top 10 ARGs (C),

709 MGEs, MRGs, and VFs (D) response to NZVI in AD.

710

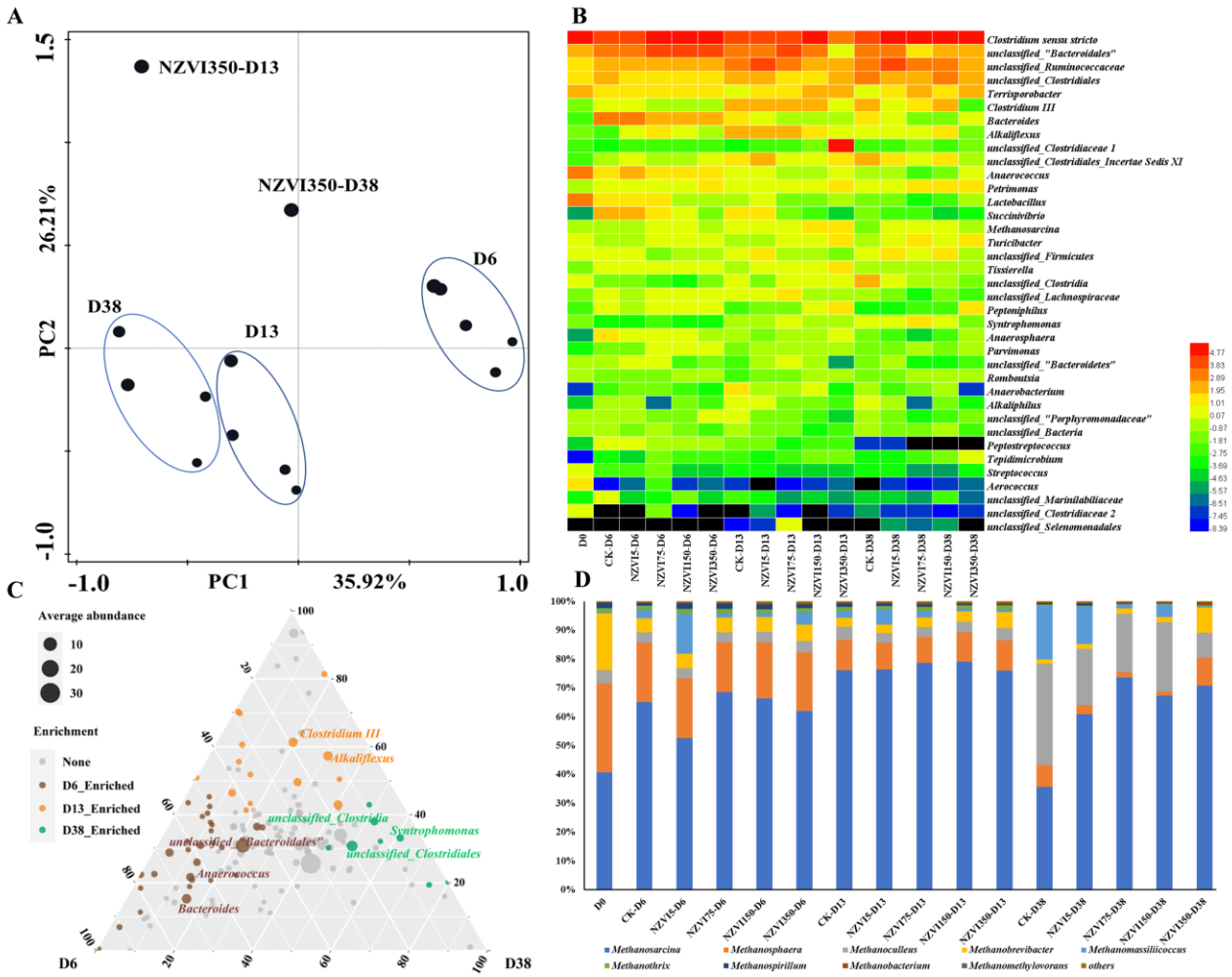

Figure 4. Principal component analysis (PCA) based on the bacterial community (A); Heatmap showing the dynamics of the top 10 genus response to NZVI (B); Ternary plot showing the enriched genus at different phases (C); Changes of the archaeal community response to NZVI in AD of swine manure (D).

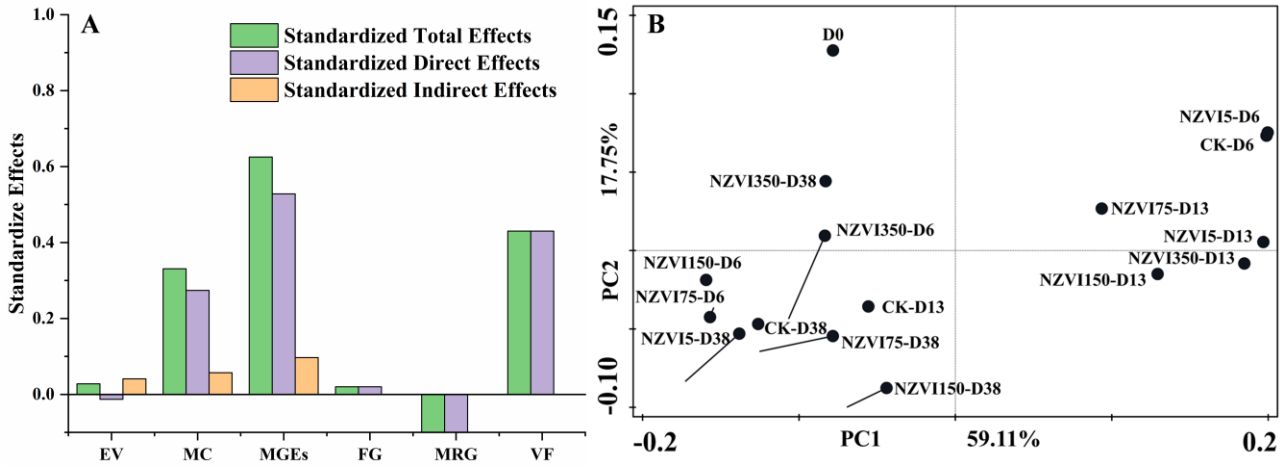

Figure 5. Structural equation models (SEM) indicating the effects of concerning factors on the changes of ARGs in AD (A); Procrustes analysis showing the relationship between ARGs and MGEs (B).

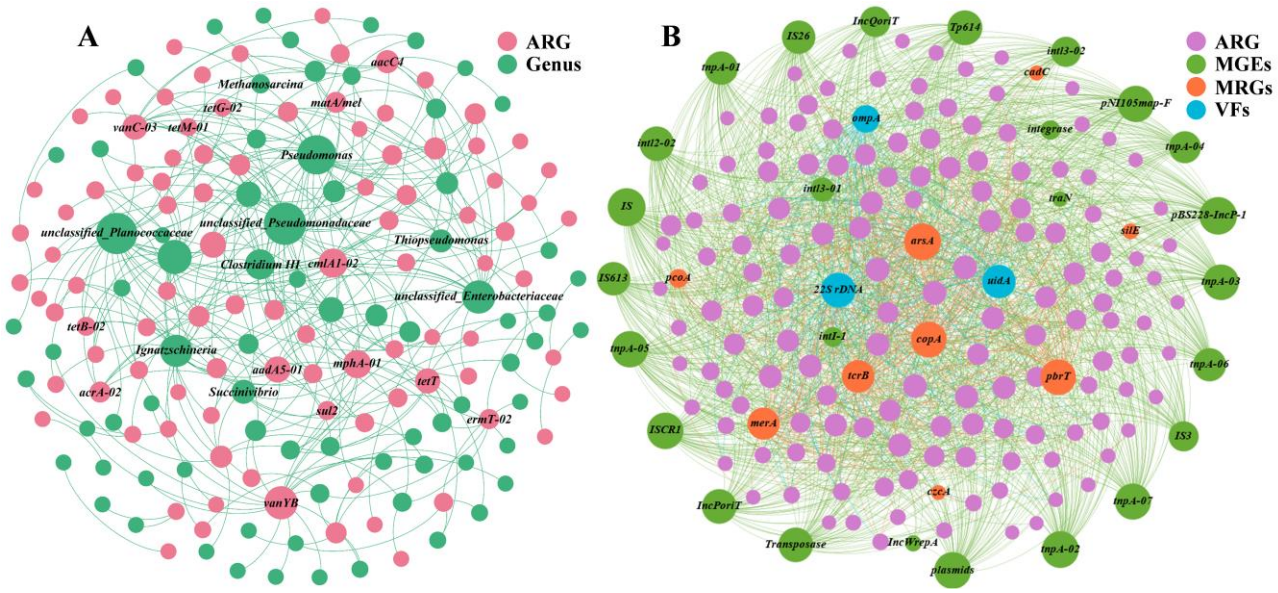

Figure 6. Network analysis (A) shows the potential hosts of ARGs, which was identified based on Spearman correlation analysis ($p<0.01$, $R^2>0.5$) between genera and ARGs subtypes; Network analysis (B) shows the relationship between ARGs and MGEs, MRGs and VFs based on the Spearman correlation analysis ($p<0.01$, $R^2>0.5$).